Smart Mater. Struct. **18** (2009) 074011 (8pp) doi:10.1088/0964-1726/18/7/074011

Control of coupled hysteretic dynamics of ferroelectric materials with a Landau-type differential model and feedback linearization

Linxiang Wang[1] **and Roderick V N Melnik**[2]

[1] Institute of Mechatronic Engineering, Hangzhou Dianzi University, Xiasha, Hangzhou 310037, People's Republic of China
[2] M^{2}NeT Laboratory, Wilfrid Laurier University, 75 University Avenue West, Waterloo, N2L 3C5, Canada

E-mail: lwang236@gmail.com and rmelnik@wlu.ca

Received 28 April 2009
Published 15 June 2009
Online at stacks.iop.org/SMS/18/074011

Abstract
In the current paper, the hysteretic dynamics and butterfly-shaped behavior of ferroelectric materials are modeled and controlled with a macroscopic differential model inspired by the Landau theory of first-order phase transformations. Hysteretic dynamic behavior of the materials is analyzed as a consequence of orientation switching and the governing equations of the dynamics are formulated as coupled differential equations describing system states switching from one equilibrium state to another. The rate dependence of hysteresis is included in the analysis. A nonlinear feedback strategy is introduced for the linearization and a simple and efficient control strategy is proposed. Comparison of the results obtained with the developed model and their experimental counterparts is presented.

(Some figures in this article are in colour only in the electronic version)

1. Introduction

For devices made from ferroelectric materials, input energy can be converted between the electrical and mechanical types by the material itself, due to the inherent property of electromechanical coupling in the materials. This fact explains the reason that ferroelectric structures and devices have been broadly employed in many engineering applications as sensor and actuators [1]. A common feature of the electromechanical dynamics of ferroelectric materials is that the input–output relations will become nonlinear with larger loading amplitudes [2–4] and hysteresis loops will occur in the E–P (electric field–electric polarization) curves under large cyclic loadings. Correspondingly, a butterfly-shaped curve will be induced in the E–ε (electric field–strain) relations. Furthermore, the hysteresis loops and butterfly curves are affected by both the mechanical and electric loading rates and their combinations [5–10].

For the purpose of analysis, control and optimization of the overall system with ferroelectric devices embedded, a challenging task is related to the modeling and control of nonlinear dynamics of ferroelectric devices. The difficulties are caused by the fact that hysteresis loops and butterfly-shaped curves are related to bifurcation phenomena in the associated dynamic systems under study and stability switchings among various equilibrium branches during the change of loadings. In such cases, the input–output relationship of the systems will not be a one-to-one relationship and will have 'memory effects' [3, 4]. In order to improve the overall performance of the system, it is essential to construct a suitable model for hysteretic dynamics. Taking into account the fact that control and analysis techniques for dynamic systems given by ordinary differential equations (ODEs) are well developed, it would be beneficial if the hysteretic dynamics can be formulated via ODE-based models. The resulting model should be able to capture the essential dynamics of the system, be simple, and has its dimension as low as possible. Another desired property of the model is that it should carry insightful information about the mechanisms of the hysteretic dynamics. The latter property of the model is particularly useful for

nonlinear analysis and control. Indeed, since there is no general nonlinear theory for this purpose, it would be helpful if the mechanisms of nonlinearities under consideration are well understood [11, 12].

Inspired by their application potentials, the dynamic models for the ferroelectric materials and structures have been a long term effort of many mathematicians, physicists, mechanical and control engineers. There are various models for the hysteresis, but very few of them describe the hysteresis and butterfly-shaped curves simultaneously in a dynamical manner [13, 14]. Modeling aspects of hysteresis itself have been under intense investigation since the beginning of the last century, particularly for the modeling of hysteresis in ferromagnetic materials using the Preisach model introduced in the 1930s [13], which have also been used extensively for other smart materials and their control [14]. Typically, however, this model deals with static hysteresis only. In order to incorporate dynamic behavior into hysteretic dynamics, the Bouc–Wen model has been used extensively based on the description of the hysteretic dynamics by a few ODEs [15], following its generalizations and the development of other models (e.g. [15–18] and references therein). However, these models remain largely empirical with the description of nonlinear material behavior based on curve fittings using the experimental data. As they carry no explicit information about the mechanism and physics of the phenomenon, their application for control and optimization purposes remains difficult.

A differential model for hysteresis in ferroic materials was also proposed in [19]. The model is based on thermodynamic considerations of phase transitions and a non-convex free energy function is constructed so that the dynamical hysteretic behavior is modeled by simulating the transition process from one physical equilibrium phase to another using thermodynamic principles and statistical mechanics. This model was also formulated in the form of ODEs where the phase change rate was expressed as a combination of the transition rates of the considered phase to other phases together with the transition rates of other phases to the considered phase. Such rates were expressed as exponential functions of a certain integral of the energy leading to additional tedious difficulties in application developments based on this model. Finally, we mention a modeling approach to hysteresis based on micromechanics of the material. In this case, the hysteretic dynamics is modeled by simulating the microstructure evolution and orientation switchings at the microscale [6–9]. Although this approach is more fundamental and carries insightful information, the modeling of microstructure evolution is often too computationally demanding to apply routinely [6–9, 20, 21], as is often required in some engineering applications. Therefore, in what follows we suggest a different approach.

Firstly we note that the hysteresis loops in the E–P curves are the consequences of orientation switching induced in the material either electrically or mechanically [2–10], while the butterfly-shaped E–ε curves can be attributed to the electromechanical coupling together with the hysteresis in the E–P curve. Our goal will be to construct a phenomenological Landau-type macroscopic model on the basis of orientation switching and then to linearize it via a nonlinear feedback strategy. In this approach, the hysteresis loops and butterfly-shaped behaviors are regarded as macroscale manifestations of orientation switching. Once an appropriate non-convex free energy function is constructed, the orientation switching dynamics can be modeled by investigating the switching dynamics of the system states from one equilibrium state to another [6, 7]. Governing equations for the switching dynamics are formulated by employing the variational principle accounting for the Rayleigh relaxation effects [20–23]. The model is expressed by two nonlinear coupled differential equations. We present results of numerical simulations where hysteretic dynamics and butterfly-shaped behaviors are successfully modeled by this model and provide a comparison of these results with their experimental counterparts. The rate-dependent characteristics are included naturally in the developed model via loading terms. Finally, a nonlinear feedback is introduced into the dynamics such that the original hysteresis can be compensated for, leading to an efficient and simple control strategy.

2. Orientation switching and hysteretic dynamics

The unique properties of the ferroelectric materials and structures can be outlined by their constitutive behavior given by the E–P and E–ε curves. It is well known that, under larger cyclic loadings, hysteresis loops occur in the E–P relations. Correspondingly, the strain induced in the materials with cyclic loadings will behave like a butterfly shape due to the nonlinear coupling effects between the electric and mechanical fields. Furthermore, the profile of the hysteresis loops and the butterfly-shaped curves will also depend on the rate of change of the loadings, leading to the rate dependence of these characteristics [2, 3].

On the basis of experimental investigations, the conclusion has been drawn that the physical essence of these unique properties of the ferroelectric materials lies with the polarization effects and orientation switching [5, 6, 10]. In fact, the hysteresis loops in the E–P relations and butterfly-shaped curves in the E–ε relations can be regarded as a macroscopic manifestation of the orientation switching. In the modeling of hysteretic dynamics of the materials, the key element is to describe the orientation switching dynamics responsible for the hysteretic behavior. As an example, in this contribution we focus on perovskite-type materials in the one-dimensional description. We assume that the material temperature is far below the transition temperature such that only tetragonal structures exist.

In the one-dimensional situation analyzed here, there are only two orientations involved, represented by the two rectangles in the horizontal direction in figure 1: the leftward and rightward orientations. The switching between the two horizontal orientations is always an 180° switching and can only be induced by the electric loadings. Taking into account the fact that in the general three-dimensional case there are six orientations involved and there are both 180° and 90° switchings induced by either electric or stress loadings, it is

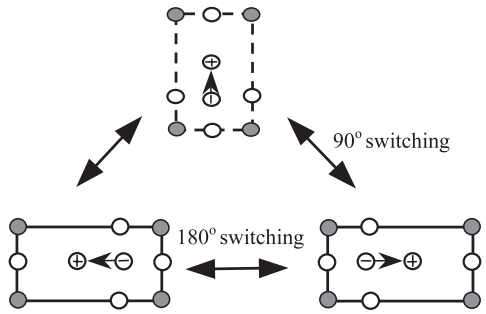

Figure 1. The sketch of one-dimensional orientation switching in ferroelectric materials.

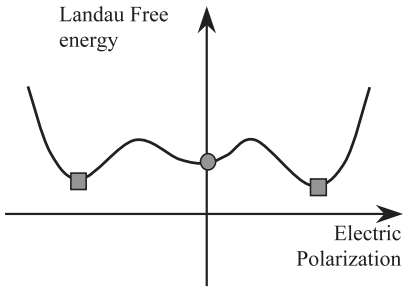

Figure 2. The Landau free energy function has three local minima.

necessary to artificially introduce one more orientation into our one-dimensional analysis in order to incorporate a 90° switching. For this purpose, a vertical orientation is introduced as outlined by the dashed rectangle in figure 1. It is worth noting that the vertical orientation introduced here is not one of the six orientations in the three-dimensional description, and it has a different free energy from the horizontal ones. It has no polarization contribution, while it has a strain contribution in the horizontal direction. The vertical orientation can be switched by either electric or stress loadings to one of the horizontal orientations, which will induce 90° switching. Via the artificial vertical orientation, the fully coupled hysteretic dynamics of the ferroelectric materials can be captured by the proposed orientation switching model. Therefore, one has three orientations in total in the current discussion, and both 180° and 90° switching can be modeled.

Following the same strategy of phenomenological theory of phase transitions, a non-convex free energy can be constructed to characterize different orientations such that each of its local equilibria can be associated with one of the orientations involved. One of the possible non-convex free energy functions for the electric field for the current orientation switching is sketched in figure 2 (the Landau free energy). The equilibria marked by the two symmetrical small rectangles are associated with the two horizontal orientations, and the central one marked by the small circle is associated with the vertical orientation.

3. Differential model

For the current system, its states are characterized by the strain (ε) and polarization (P), respectively. The loadings are the electrical field (E) and mechanical stress (σ). Both ε and P are assumed to be uniform in the considered structure since the focus of the current paper is to model and control the macroscale low-dimensional dynamics of the materials, rather than to simulate the microstructure evolution associated with the polarizations and orientation switching in the material. Therefore, there is no need to consider any spatial variation of the variables. The governing equations for the system states' evolution can be obtained by simulating the transition process of the system states from one local minimum to another.

The kinetic energy of the system can be formulated in the following form:

$$U = \frac{1}{2}\left(I_P\left(\frac{\mathrm{d}P}{\mathrm{d}t}\right)^2 + I_\varepsilon\left(\frac{\mathrm{d}\varepsilon}{\mathrm{d}t}\right)^2\right), \tag{1}$$

where I_P and I_ε are coefficients accounting for the inertial effects of the transition in the electric and mechanical fields, respectively. P is the primary order parameter and ε is the secondary order parameter.

The potential energy V can be taken as follows:

$$V = L\left(\frac{a_2}{2}P^2 + \frac{a_4}{4}P^4 + \frac{a_6}{6}P^6 + \frac{k}{2}\varepsilon^2 + \frac{b}{2}\varepsilon P^2 - EP - \sigma\varepsilon\right), \tag{2}$$

where a_2, a_4, a_6, k and b are material constants and L is the length of the considered one-dimensional structure. L can be set to 1 without losing generality. The above energy is taken as the integral of the Gibbs free energy function over the considered structure, which is a non-convex function constructed on the basis of the Landau free energy function [24–26]. The first three terms together gives non-convex energy (the Landau type) as sketched in figure 2. The fourth term models the elastic energy contributions, the fifth term models the coupling effects between the mechanical and electric fields, while the last two terms model the energy contributions related to the external electric and mechanical loadings.

In order to take into account the relaxation effects of the orientation switching processes, the Rayleigh dissipation effect is introduced as

$$R = -\frac{1}{2}\left(\tau_P\left(\frac{\mathrm{d}P}{\mathrm{d}t}\right)^2 + \tau_\varepsilon\left(\frac{\mathrm{d}\varepsilon}{\mathrm{d}t}\right)^2\right), \tag{3}$$

where τ_P and τ_ε are material-specific constants. The negative sign indicates that it is a dissipative term.

Using the Euler–Lagrange equation, the governing equations of the considered dynamics can be formulated as the following temporal evolution equations for P and ε:

$$\begin{aligned} I_P\frac{\mathrm{d}^2P}{\mathrm{d}t^2} + \tau_P\frac{\mathrm{d}P}{\mathrm{d}t} + a_2P + a_4P^3 + a_6P^5 + b\varepsilon P - E = 0, \\ I_\varepsilon\frac{\mathrm{d}^2\varepsilon}{\mathrm{d}t^2} + \tau_\varepsilon\frac{\mathrm{d}\varepsilon}{\mathrm{d}t} + k\varepsilon + \frac{bP^2}{2} - \sigma = 0. \end{aligned} \tag{4}$$

The above second-order equations describe the evolution of polarization and strain upon external loadings. They include

both the inertial effects and relaxation effects. The model points out that the system states will keep evolving in such a way that their total energy will be gradually minimized. In its essence, the evolution law of the (macroscopic) system is reminiscent of that modeled with the time-dependent Ginzburg–Landau (TDGL) equation applied at the mesoscopic level [4, 6, 24]. However, here the governing equations for both the electric and mechanical fields are given by a coupled system of second-order differential equations.

If the loading process is very slow compared to the time constants such that the system states can be considered in their equilibrium states, both the inertial and relaxation effects can be neglected, and from (4) we can obtain the coupled constitutive laws for the considered materials by setting all the time derivative terms to zero:

$$E = a_2 P + a_4 P^3 + a_6 P^5 + b\varepsilon P, \qquad \sigma = k\varepsilon + \frac{bP^2}{2}. \tag{5}$$

In the above constitutive laws, the mechanical and electric fields are nonlinearly coupled. The dynamic response of the system (4) could have overshot when phase transitions take place, while experimental observations indicate frequently that the dynamic response is over-damped and has no overshoot, even when orientation switching is induced [3, 6]. This fact makes it possible to simplify the system given by (4) further, leaving out the derivatives higher than one by neglecting inertial effects:

$$\tau_P \frac{\mathrm{d}P}{\mathrm{d}t} + a_2 P + a_4 P^3 + a_6 P^5 + b\varepsilon P - E = 0, \qquad \tau_\varepsilon \frac{\mathrm{d}\varepsilon}{\mathrm{d}t} + k\varepsilon + \frac{bP^2}{2} - \sigma = 0. \tag{6}$$

The above simplification agrees with experimental observations that the inertial effects of the orientation switching are normally much smaller compared to the relaxation effects.

4. Feedback linearization

Since the techniques for dynamic analysis and controller design for systems given by linear ordinary differential equations are well established, one of the ways to approach the problem of control in our case is to see if the hysteretic dynamic can be approximated by or associated with a specific linear system. A conventional methodology, based on an approximation of nonlinear systems via Taylor expansion series, faces difficulties in this case since we have to deal with structure nonlinearities accompanied by bifurcation phenomena in system dynamics [11, 12]. Therefore, in what follows we suggest a different approach based on a nonlinear feedback such that the original hysteresis is compensated for and the original system can be effectively linearized.

The essence of the feedback linearization of the state equations we pursue here is to introduce a feedback which is a nonlinear function of the system states. The nonlinear factors induced by this feedback will play a role aiming at compensating the original nonlinear factor. First, we recast our

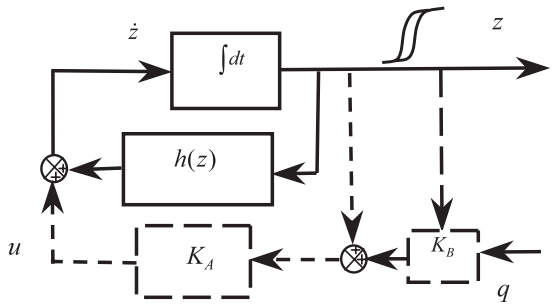

Figure 3. Diagram sketch of the feedback linearization strategy for the hysteretic dynamics of ferroelectric structures.

model (6) into the following state space form with separated linear and nonlinear parts:

$$\boldsymbol{\tau}\dot{\mathbf{z}} = \mathbf{l}(\mathbf{z}) + \mathbf{h}(\mathbf{z}) + \mathbf{u},$$
$$\boldsymbol{\tau} = \begin{bmatrix} \tau_P & 0 \\ 0 & \tau_\varepsilon \end{bmatrix}, \qquad \mathbf{z} = \begin{bmatrix} P \\ \varepsilon \end{bmatrix}, \qquad \mathbf{u} = \begin{bmatrix} E \\ \sigma \end{bmatrix},$$
$$\mathbf{l}(\mathbf{z}) = \mathbf{K}_P \mathbf{z} = \begin{bmatrix} -a_2 & 0 \\ 0 & -k \end{bmatrix} \mathbf{z}, \tag{7}$$
$$\mathbf{h}(\mathbf{z}) = -\begin{bmatrix} a_4 P^3 + a_6 P^5 + b\varepsilon P \\ \frac{bP^2}{2} \end{bmatrix},$$

where $\mathbf{l}(\mathbf{z})$ is the linear part and $\mathbf{h}(\mathbf{z})$ is the nonlinear part. The above system will have a hysteretic response in both P and ε. For the feedback linearization purpose, a new input $\mathbf{q} = [E_n(t), \sigma_n(t)]^{\mathrm{T}}$ is introduced as the new input for the linear system obtained via feedback linearization. Assume that the original input $\mathbf{u} = [E(t), \sigma(t)]^{\mathrm{T}}$ can be decomposed into two components, as sketched by the block diagram connected with dashed lines in figure 3. The feedback law can be constructed by using nonlinear functions of the system state (P, ε) and the new input $\mathbf{q}$ as follows:

$$\mathbf{u} = \mathbf{K}_{\mathrm{A}}(P, \varepsilon) + \mathbf{K}_{\mathrm{B}}(P, \varepsilon)\mathbf{q}, \tag{8}$$

where $\mathbf{K}_{\mathrm{A}}$ and $\mathbf{K}_{\mathrm{B}}$ are two operator vectors to be determined on the system states. The goal of the nonlinear feedback is then to transform the nonlinear system given by (7) to a linear one as follows:

$$\boldsymbol{\tau}\dot{\mathbf{z}} = \mathbf{A}\mathbf{z} + \mathbf{M}\mathbf{q}, \tag{9}$$

where $[\mathbf{A}, \mathbf{M}]$ is a matrix pair of a controllable linear system, as sketched in figure 4. In applications, the pair $[\mathbf{A}, \mathbf{M}]$ is chosen from the considerations of system stability, system performance, convenience, control cost and other criteria. In order to illustrate our idea here, the $[\mathbf{A}, \mathbf{M}]$ pair is chosen such that the system (9) turns into a simple decoupled system as follows:

$$\frac{\mathrm{d}P}{\mathrm{d}t} = -P + E_n, \qquad \frac{\mathrm{d}\varepsilon}{\mathrm{d}t} = -\varepsilon + \sigma_n. \tag{10}$$

In this case, we have

$$\mathbf{A} = -\begin{bmatrix} \tau_P & 0 \\ 0 & \tau_\varepsilon \end{bmatrix}, \qquad \mathbf{M} = \begin{bmatrix} \tau_P & 0 \\ 0 & \tau_\varepsilon \end{bmatrix}. \tag{11}$$

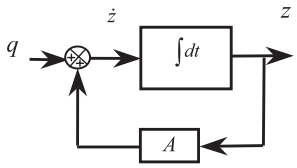

Figure 4. The corresponding linear systems associated with the feedback linearization of the hysteretic dynamics of the ferroelectric structures.

By substituting the feedback law (8) into (9), it is easy to deduce that

$$\boldsymbol{\tau}\dot{\mathbf{z}} = \mathbf{A}\mathbf{z} + \mathbf{M}\mathbf{K}_{\mathrm{B}}^{-1}(\mathbf{u} - \mathbf{K}_{\mathrm{A}}), \tag{12}$$

where $\mathbf{K}_{\mathrm{B}}^{-1}$ is the inverse of the operator $\mathbf{K}_{\mathrm{B}}$. By comparing (12) with (7), a simple calculation gives the following relations:

$$\mathbf{A}\mathbf{z} - \mathbf{M}\mathbf{K}_{\mathrm{B}}^{-1}\mathbf{K}_{\mathrm{A}} = \mathbf{K}_P\mathbf{z} + \mathbf{h}(\mathbf{z}), \qquad \mathbf{M}\mathbf{K}_{\mathrm{B}}^{-1} = \mathbf{I}. \tag{13}$$

With the $[\mathbf{A}, \mathbf{M}]$ pair chosen as in (11), the operators for the nonlinear feedback can be calculated as follows:

$$\mathbf{K}_{\mathrm{A}} = (\mathbf{A} - \mathbf{K}_P)\mathbf{z} - \mathbf{h}(\mathbf{z}) = \begin{bmatrix} -\tau_P + a_2 & 0 \\ 0 & -\tau_\varepsilon + k \end{bmatrix} \begin{bmatrix} P \\ \varepsilon \end{bmatrix} + \begin{bmatrix} a_4 P^3 + a_6 P^5 + b\varepsilon P \\ \frac{bP^2}{2} \end{bmatrix}, \tag{14}$$

$$\mathbf{K}_{\mathrm{B}} = \mathbf{M} = \begin{bmatrix} \tau_P & 0 \\ 0 & \tau_\varepsilon \end{bmatrix}.$$

It is easy to see that the introduced feedback law (8) with $[\mathbf{K}_{\mathrm{A}}, \mathbf{K}_{\mathrm{B}}]$ given in (14) is responsible for a hysteretic component, as indicated by nonlinear terms in $\mathbf{K}_{\mathrm{A}}$. Note also that it has an opposite sign to the original nonlinear terms. The original hysteretic dynamics is therefore canceled by the one introduced via feedback, such that the output of the hysteretic dynamics system can be regarded as that of a corresponding linear system with a new input.

Since the correspondence between the linear system (9) and the original hysteretic one (7) is given by analytical deterministic expressions, it is possible to perform the control system analysis and design by using the linear model (9) and determine the input $\mathbf{q}$ to drive the system in a desired trajectory. By using (9) and (14), it is straightforward to obtain the input in terms of E and σ for the hysteretic dynamics (7). Hence, by using the above approach, the difficulties caused by the hysteresis in the control system can be overcome.

Before moving to representative numerical examples, we note that the success of the proposed methodology is based on (a) a differential model for hysteretic dynamics we have to deal with and (b) the analytical form of the relationship between the transformed and original systems. Finally we note that, while the nonlinear feedback strategy can also be applied for the linearization of the input–output relations as is well known from the literature [11, 12], our discussion here has been focusing on the nonlinear feedback strategy for the linearization of the state equations.

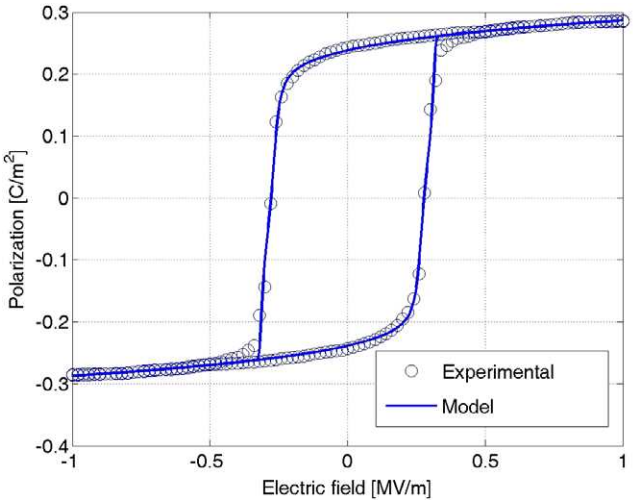

Figure 5. Comparison of modeled and measured E–P curves.

5. Numerical results

5.1. Coupled hysteretic dynamics

First, we demonstrate the capability of the proposed model. We base our consideration on equations (6) (for other modeling details of hysteresis and butterfly effects in the ferroelectric materials we refer the reader to [23]). The parameter values in our calculations are taken as follows [23]: $\tau_p = 0.01$, $a_2 = -1.06$, $a_4 = -51\,001.48$, $a_6 = -1797.95$, $b = -2580.16$, $k = 65.42$ and $\tau_\varepsilon = 0$ (see the physical units in [10, 23]). In the example that follows, the only loading applied to the system was $E = \sin 2\pi t$ (the applied mechanical stress was set to zero).

The simulated E–P and E–ε curves using the estimated parameter values are compared with their experimental counterparts in figures 5 and 6. Experimental data is read from the experimental curves in [10] and re-plotted here as a dashed line marked with small cycles. The comparison shows that the modeled hysteresis agrees very well with the experimental one. The modeled butterfly-shaped E–ε curve also agrees with its experimental counterpart, although this latter result can be improved further. These results demonstrate the capability of the proposed differential model to model the hysteresis and butterfly-shaped behaviors in a coupled manner. Note that the current parameter values provided an estimation with more bias towards the polarization compared to the strain. This explains why the agreement between the modeled and experimental results in the E–P curves is better compared to the E–ε curve. Similar to [23], it can be shown that better estimates via the fitness of the model with experimental data would lead to increased accuracy.

5.2. Rate dependence

As mentioned, the rate dependence of the hysteretic dynamics is included in the proposed model. This can be observed from (6): the loading $E(t)$ is included in the formulation of the model so that the output of the system will be influenced

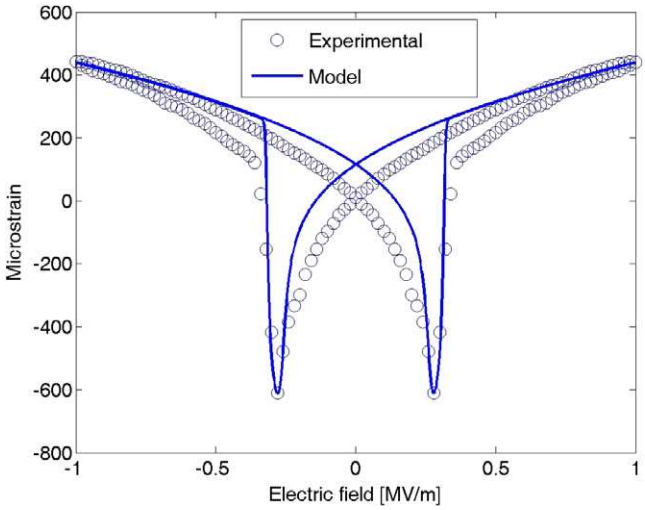

Figure 6. Comparison of modeled and measured E–ε curves.

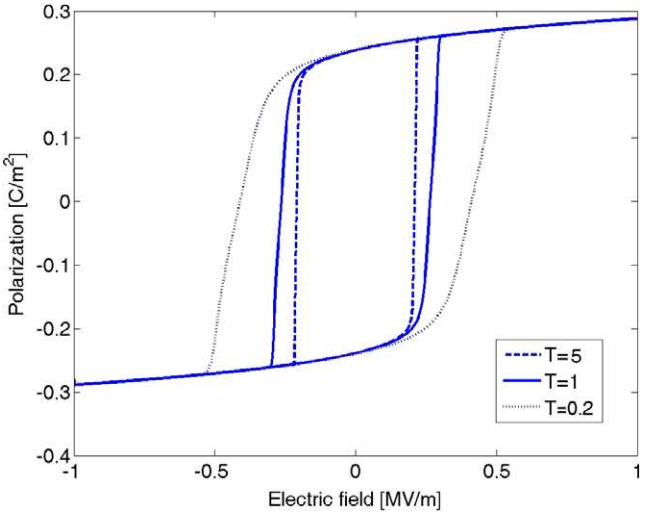

Figure 7. Comparison of modeled and measured E–P curves.

by the rate of loading change. To illustrate this feature, the loading $E(t)$ is applied to the system with several different rates of change. For the entire loading period T, $E(t)$ starts from the minimal value (-1 MV m^{-1}), increases linearly to the maximal value (1.0 MV m^{-1}) at $t = T/2$ and then decreases linearly to the minimal value again at $t = T$. The loading period T is chosen as $T = 0.2$, 1 and 5 s, respectively. All other parameters remain unchanged.

For comparison, in figures 7 and 8 we present the simulated P and ε by using (6) with different T. We observe that the output of the system is substantially influenced by the rate of loading change. When the loading period T is small, the applied electric field changes fast and the orientation switching needs time to relax. As a result, it cannot catch up with the change of the electric field. This extra delay affects the simulated polarization and strain, resulting in smoothing out a jump caused by the orientation switching in the E–P and E–ε curves. However, when the loading period is larger (e.g. chosen $T = 5$), the rate of change of the electric field is rather small and the orientation switching has enough time to be completed. The polarization has enough time to relax and achieve its equilibrium state. In this case, a jump caused by the orientation switching is more pronounced, as seen in sharper profiles of the simulated polarization and strain curves. The numerical results show that the orientation switching dynamics has the behavior similar to the behavior of dynamic systems with damping factors.

5.3. Linearized dynamics

For the dynamic analysis and control of ferroelectric structures and devices, one of the most challenging parts is to determine the necessary inputs to drive the system in a certain way desired by the control target, due to the existence of the hysteresis associated with the memory effects. Here, numerical simulations are presented to demonstrate that, by using the nonlinear feedback linearization strategy discussed above. The correct inputs to the hysteretic system (7) can be easily

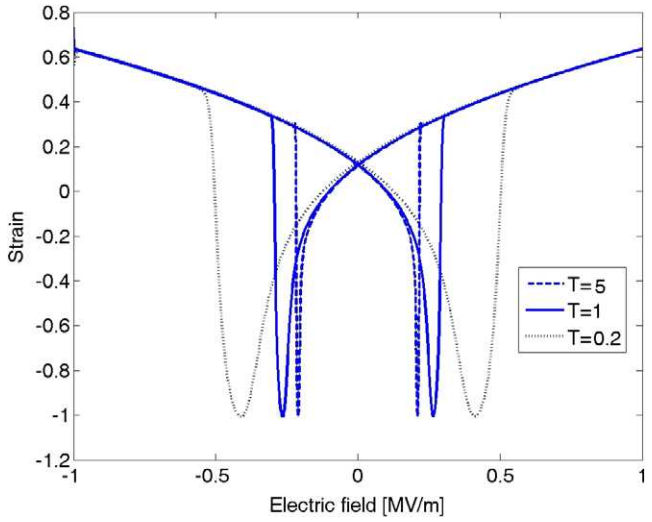

Figure 8. Comparison of modeled and measured E–ε curves.

obtained by using the feedback law given in (8) and (14), based on determining the associated inputs of the linear system (9).

Since the hysteretic dynamics of ferroelectric structures is caused by the orientation switching, only the governing equation for the polarization evolution is considered here to illustrate the main idea. By setting the term with the strain to zero in the first equation in (6), the model can be simplified as follows:

$$\tau_P \frac{\mathrm{d}P}{\mathrm{d}t} = -(a_2 P + a_4 P^3 + a_6 P^5) + E. \qquad (15)$$

Next, we assume that the initial polarization is $P = -0.3$ C m^{-2} at $t = 0$ and we would like to drive the system exponentially to the state $P = 0.3$ C m^{-2} at $t = t_1$, and then drive it exponentially back to the states $P = -0.3$ C m^{-2} at $t = t_2$. The values of t_1 and t_2 are specified according to the system control requirements; so does the exponential law for the evolution of the polarization and the target P values. As an example, we choose $t_1 = 4$, $t_2 = 8$ and the exponential law

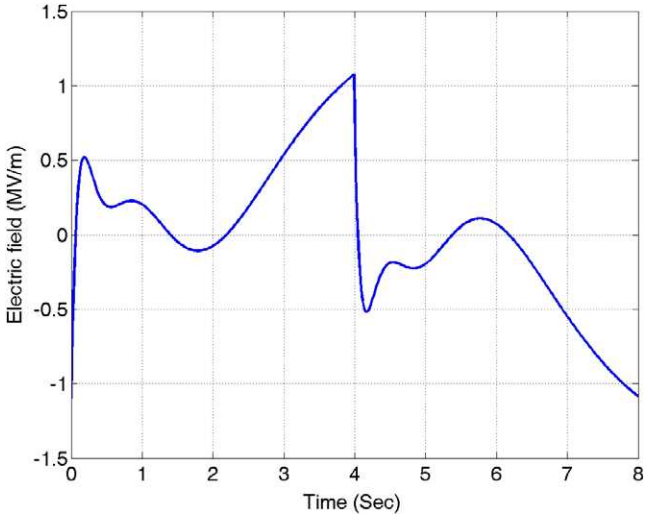

Figure 9. The input to the hysteretic system in order to drive the system in a desired trajectory.

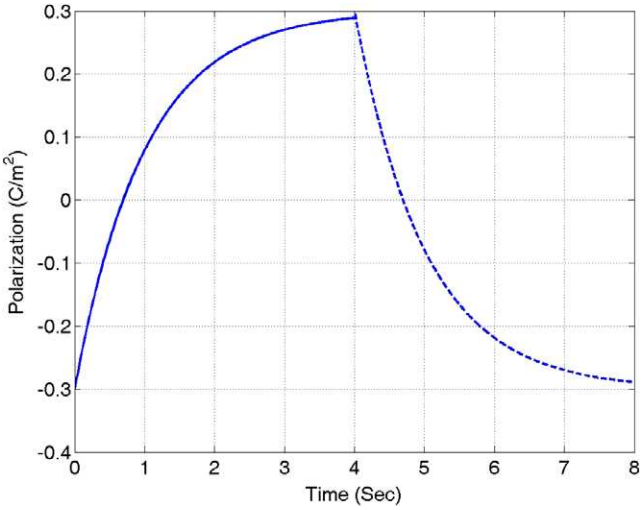

Figure 10. The trajectory of the hysteretic system with the designed input.

has been chosen by $\exp(-t)$. The task now is to determine the actual input $E(t)$ for the system (15).

First we note that, based on the above discussion, $E(t)$ can be decomposed into two parts as follows:

$$E = K_{\mathrm{A}}(P) + K_{\mathrm{B}}(P)E_n. \tag{16}$$

Since the exponential evolution law for P is specified above, and the time constraints are specified by t_1 and t_2, the control pair $[\mathbf{A}, \mathbf{M}]$ in (9) can be chosen as $[-\tau_P, \tau_P]$ for the current example, such that the linear system takes the following form:

$$\frac{\mathrm{d}P}{\mathrm{d}t} = -P + E_n. \tag{17}$$

It is easy to see that, under constant loading $E_n(t) = 0.3$, (17) will drive $P(t)$ exponentially to 0.3, while constant loading $E_n(t) = -0.3$ will do the opposite, leading to the exponential evolution law, $P(t) = \exp(-t)$, as required. A simple calculation leads us to the following relationships:

$$K_{\mathrm{A}} = -\tau_P P + a_2 P + a_4 P^3 + a_6 P^5, \qquad K_{\mathrm{B}} = \tau_P. \tag{18}$$

By using (16) and (18), one can easily calculate the right input $E(t)$ for (15) to drive the system in the desired trajectory. For the current example, the calculated input is plotted in figure 9 as a function of time. The actual response of (15) is simulated with the calculated input and is plotted in figure 10. Observe that the state of the hysteretic system is driven precisely in an exponential manner as required by the input signal calculated via the linearization strategy. The output is exactly the same as the one obtained with (17) under E_n, which is a classical first-order linear dynamics.

In figure 11 the effects of the nonlinear feedback strategy are shown by plotting the output of (15) as a function of $E(t)$. Observe that the input–output relation of (15) still exhibits hysteretic behavior. This behavior is more complicated compared to the one presented in figure 7 since the output has been specified according to the system control requirements.

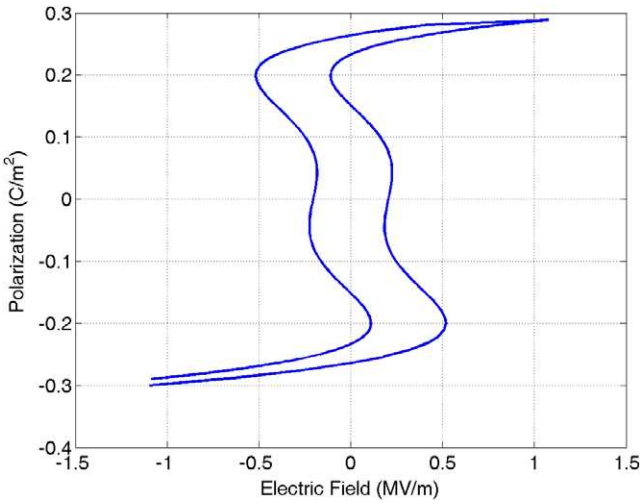

Figure 11. The hysteretic responses of ferroelectric structures under a changing electric field.

Indeed, for the purpose of control of the hysteretic dynamics, the input into the system can always be decomposed into two parts: one is the nonlinear feedback part which aims at canceling the hysteresis in the original dynamics, while the other part is the requirement input to drive the associated linearized system in a certain manner. In other words, the hysteretic part of the original dynamics is compensated by the hysteretic behavior introduced by the nonlinear feedback, as part of the input. The developed strategy substantially simplifies the control system design for hysteretic systems.

6. Conclusion

We have presented a coupled macroscale model describing the hysteresis and butterfly effects in ferroelectric materials based on the phenomenological theory of orientation switching. We have demonstrated its effectiveness in modeling the hysteretic dynamics and electromechanical coupling

effects in ferroelectrics and provided a comparison between computational and experimental results. We have introduced a nonlinear feedback strategy for the linearization of the model and developed a simple and efficient control strategy.

Acknowledgments

LW acknowledges the support of the National Natural Science Foundation of China (grant no. 10872062) and the Natural Science Foundation of Zhejiang Province, China (grant no. Y1080462). RM acknowledges the support from the NSERC, CRC and SHARCNET Programs.

References

[1] Arnau A 2004 *Piezoelectric Transducers and Applications* (Berlin: Springer)
[2] Hall D A 2001 Nonlinearity in piezoelectric ceramics *J. Mater. Sci.* **36** 4575–601
[3] Smith R C 2005 *Smart Material Systems: Model Development* (Philadelphia, PA: SIAM)
[4] Wang L X, Liu R and Melnik R V N 2009 Modeling large reversible electric-field-induced strain in ferroelectric materials using 90 degrees orientation switching *Sci. China Ser.* E **52** 141–7
[5] Lynch C S 1996 The effect of uniaxial stress on the electro-mechanical response of 8/65/35 PLZT *Acta Mater.* **44** 4137–48
[6] Ahluwalia R, Lookman T, Saxena A and Cao W 2005 Domain-size dependence of piezoelectric properties of ferroelectrics *Phys. Rev.* B **72** 014112
[7] Landis C M, Wang J and Sheng J 2004 Microelectromechanical determination of the possible remanent strain and polarization states in polycrystalline ferroelectrics and the implications for phenomenological constitutive theories *J. Intell. Mater. Syst. Struct.* **15** 513–25
[8] Hwang S C, Lynch C S and McMeeking R M 1995 Ferroelectric/ferroelastic interactions and a polarization switching model *Acta Metall. Mater.* **43** 2073–84
[9] Kamlah M 2001 Ferroelectric and ferroelastic piezoceramics—modeling of electromechanical hysteresis phenomena *Contin. Mech. Thermodyn.* **13** 219–68
[10] Brown S A, Hom C H, Massuda M, Prodey J D, Bridger K, Shankar N and Winzer S 1996 Electromechanical testing and modeling of a $Pb(Mg_{1/3}Nb_{2/3})$–$PbTiO_3$–$BaTiO_3$ relaxor ferroelectric *J. Am. Ceram. Soc.* **79** 2271–82
[11] Sastry S 1999 *Nonlinear Systems: Analysis, Stability, and Control* (New York: Springer)
[12] Khalil H K 2004 *Nonlinear Systems* (Englewood Cliffs, NJ: Prentice-Hall)
[13] Mayergoyz I D 2003 *Mathematical Models of Hysteresis and their Applications* (New York: Elsevier)
[14] Gorbet R B and Morris K A 2003 Closed-loop position control of Preisach hystereses *J. Intell. Mater. Syst. Struct.* **14** 483–95
[15] Wen Y K 1976 Method for random vibration of hysteretic systems *J. Eng. Mech.* **102** 249–63
[16] Visintin A 1995 *Differential Models of Hysteresis* (Berlin: Springer)
[17] Ikhouane F, Hurtado J E and Rodellar J 2007 Variation of the hysteresis loop with the Bouc–Wen model parameters *Nonlinear Dyn.* **48** 361–80
[18] Awrejcewicz J, Dzyubak L and Lamarque C H 2008 Modelling of hysteresis using Masing–Bouc–Wen's framework and search of conditions for the chaotic responses *Commun. Nonlinear Sci. Numer. Simul.* **13** 939–58
[19] Smith R C, Seelecke S, Dapino M and Ounaies Z 2006 A unified framework for modeling hysteresis in ferroic materials *J. Mech. Phys. Solids* **52** 46–85
[20] Wang L X and Melnik R V N 2008 Modifying macroscale variant combinations in 2D structure using mechanical loadings during thermally induced transformation *Mater. Sci. Eng.* A **481/482** 190–3
[21] Wang L X and Melnik R V N 2008 Simulation of phase combinations in shape memory alloys patches by hybrid optimization methods *Appl. Numer. Math.* **58** 511–24
[22] Wang L X, Liu R and Melnik R V N 2008 Feedback linearization of hysteretic thermoelastic dynamics of shape memory alloy actuators with phase transformations *Adv. Mater. Res.* **47–50** 69–72
[23] Wang L X, Chen Y and Zhao W L 2008 Macroscopic differential model for hysteresis and butterfly-shaped behavior in ferroelectric materials *Adv. Mater. Res.* **47–50** 65–8
[24] Chen L Q 2008 Phase field methods of phase transitions/domain structures in ferroelectric thin films: a review *J. Am. Ceram. Soc.* **91** 1835–44
[25] Falk F 1980 Modelling free energy, mechanics, and thermomechanics of shape memory alloys *Acta Metall.* **28** 1773–80
[26] Falk F and Konopka P 1990 Three-dimensional Landau theory describing the martensitic phase transformation of shape memory alloys *J. Phys.: Condens. Matter* **2** 61–77